Water Supply

Water Supply Vol 22 No 9, 7281 doi: 10.2166/ws.2022.313

The dynamic identification mechanism research of drought based on process description

Li Shaoxuan, Xie Jiancang, Yang Xue*, Xue Ruihua and Zhao Peiyuan

State Key Laboratory of Eco-hydraulics in Northwest Arid Region, Xi'an University of Technology, Xi'an 710048, Shaanxi, China
*Corresponding author. E-mail: xue.yang@xaut.edu.cn

ABSTRACT

Drought is one of the most common natural disasters, which can cause heavy losses on a global scale. Strengthening the research on drought identification mechanism has an important guiding role in drought disaster prevention and mitigation. The current drought identification is mostly static in the process of drought, and there is a problem that the historical evaluation information and the drought prediction information are not closely combined, with limited application value. Based on the physical cumulative and recessional effects of drought events, this paper further uses the Standardized Precipitation Index (SPI) to divide the whole drought process into four stages: accumulation → outbreak → reaction → restoration. In addition, this study proposes a new dynamic identification mechanism based on drought process, and develops a drought prediction model combining singular spectrum analysis and BP neural network (SSA-BPNN), filling the gap between scientific research and practical application. Using three drought events in the Yulin region of China as examples for simulation studies, the results show that the use of the new mechanism can not only improve the application value of the SSA-BPNN model, but also effectively advance the drought preparation time and resistance level.

Key words: case simulation, division of drought stages, drought process description, dynamic identification mechanism

HIGHLIGHTS

- The described drought events process is based on Hurst phenomenon.
- SPI was used to divide the stages of drought process.
- A dynamic identification mechanism of drought events was constructed.
- Case simulation was carried out to verify the drought events dynamic identification mechanism.

GRAPHICAL ABSTRACT

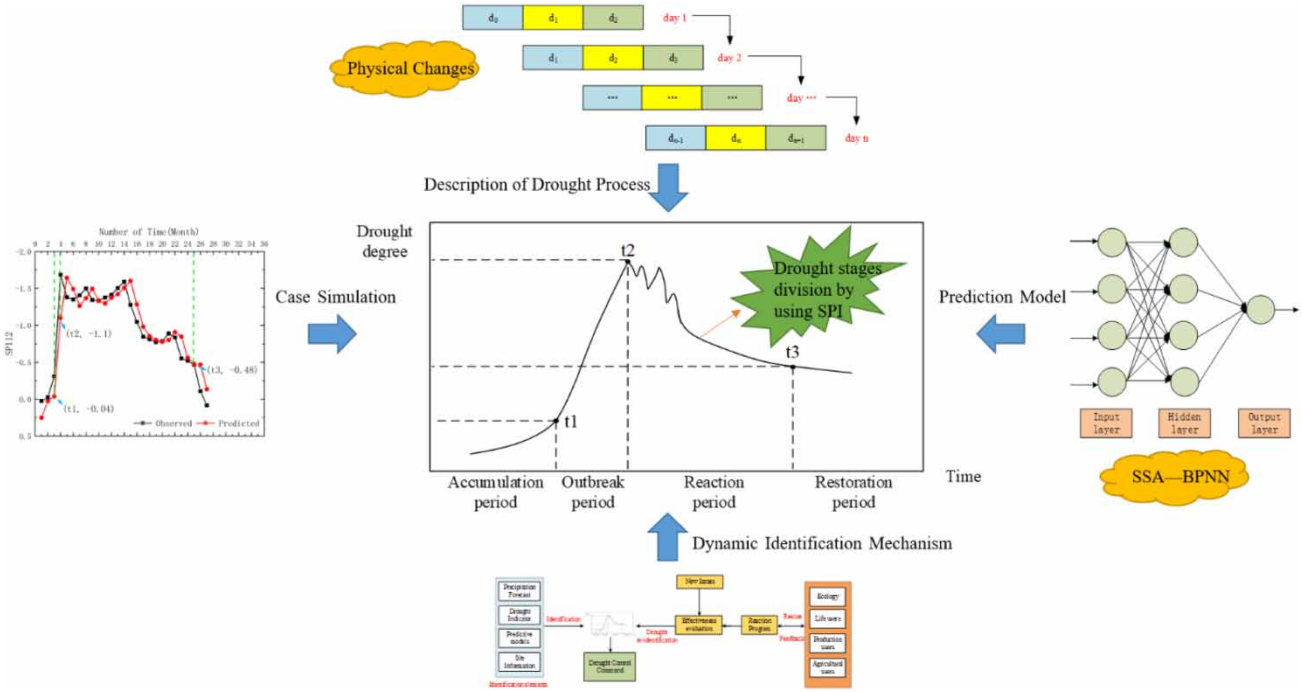

1. INTRODUCTION

Droughts appear more frequently because of extreme weather in recent years, with increasing losses in economy and lives. Therefore, drought identification and warning have attracted more attention in recent decades, and identifying drought based on classification is the most popular approach. From a different field's perspective, drought can be separated into meteorological drought (Singh *et al.* 2021), agricultural drought (Zhang *et al.* 2021), hydrological drought (Kolachian & Saghafian 2021), and socioeconomic drought (Kundu *et al.* 2021). The release of drought warning signals is based on drought identification, which requires scientific quantitative calculation indices. The identification results obtained through visual observation or human subjective judgment are unreasonable and inaccurate.

Motivated by improving the accuracy of drought identification, more than 100 indices to quantify the drought severity are proposed (Ali *et al.* 2019), as well as the threshold values for classification (Ding *et al.* 2021). Some frequently used indices include the Percent of Normal Index (PNI) (Zargar *et al.* 2011), Z-Score Index (ZSI) (Wu *et al.* 2001), Reconnaissance Drought Index (RDI) (Tsakiris & Vangelis 2005), Palmer Drought Severity Index (PDSI) (Palmer 1965), Standardized Precipitation Index (SPI) (McKee *et al.* 1993), Standardized Precipitation Evapotranspiration Index (SPEI) (Vicente-Serrano *et al.* 2014), and remote sensing drought index etc. Nikbakht *et al.* (2013) used PNI to analyze the severity of streamflow drought in northwestern Iran, and detected the time trend of the severity of streamflow drought. Sridhara *et al.* (2021) used ZSI, PNI, SPI and other drought indices to identify and evaluate the drought situation in Chitradurga district of Karnataka, India from 1967 to 2017, and the evaluation results were used to combat the impact of drought. Marini *et al.* (2019) investigated the spatiotemporal drought characteristics in Puglia region, Italy, based on the SPI and RDI from 1960 to 2013, and compared the differences between these two indices in characterizing drought. Javed *et al.* (2020) studied drought evolution and spatiotemporal changes under different land cover types in China from 1982 to 2017 based on two remote sensing indices, Normalized Difference Vegetation Index (NDVI) (Tucker 1979) and Vegetation Condition Index (VCI) (Kogan 1990), as well as meteorological index SPI. Berliana *et al.* (2021) used PDSI identification to analyze the dry and wet seasons of Java Island. Pramudya & Onishi (2018) applied SPI to analyze the extent and duration of drought in Tegal City, Indonesia, in 2015. Dar & Dar (2021) applied SPI-3 to study the temporal and spatial variability of drought in India and its impact on agriculture.

Summarizing these studies, the drought identification indices correspond to the whole drought event, which means the identification is somehow an after-event evaluation. While drought is a time accumulative process, identifying the drought

severity in a process is more scientifically valid. Therefore, Yun *et al.* (2012) studied the drought process from July 2009 to May 2010 in Qianxinan Prefecture, Guizhou Province, China, and divided the evolution process from emergence to disappearance of drought into six stages. However, in general, studies on drought process identification are limited in literature, and these studies focus on elements such as the identification of the number of drought processes over a period of time. For example, Cai *et al.* (2021) used the regional drought process identification method to effectively identify a total of 75 regional drought processes in North China from 1960 to 2019, and evaluated the drought process from multiple perspectives. Wang *et al.* (2021) used the daily temperature and rainfall data from eight meteorological stations in Haixi Prefecture, Qinghai Province from 1981 to 2020, identified 192 drought processes based on Meteorological Drought Composite Index (MCI), and explored the changing characteristics of their disaster causing factors.

Since current drought identification research is based on historical information, it means that the identification results cannot really help to decrease the drought losses in pre-warning application. As suggested by Sutanto *et al.* (2020), one of the most effective strategies to reduce drought losses is to issue timely and targeted warnings to end users one month to several seasons in advance. To achieve this aim, some studies tried to predict the drought indices to provide information for drought warning. For instance, Shin *et al.* (2020) used PDSI to build a Bayesian network-based drought prediction model (BNDF-DP) to provide water resources managers with the ability to flexibly respond to adverse drought risks and formulate drought mitigation action plans. Altunkaynak & Jalilzadnezamabad (2021) applied PDSI to build a drought prediction model based on discrete wavelet transform (DWT) combined with fuzzy, K-Nearest Neighbor (KNN) and Support Vector Machine (SVM) to formulate a drought preparedness plan and mitigation measures in advance. Ghasemi *et al.* (2021) used Multilayer Perceptron (MLP) neural network, General Regression Neural Network (GRNN) neural network and Gaussian process regression to three machine learning models to forecast the annual drought index SPEI12 of 79 Iranian weather stations 1–3 months in advance, which greatly helped the agricultural sector to reduce the negative effects of drought. Nasir & Hamdan (2021) used SPI6 and SPI24 to build a Recurrent Neural Network (RNN) model to predict the degree of drought in Iraq from 2020 to 2030, and played an important guiding role in Iraq's future water resources planning and management. However, these drought predictions could only provide some information for an issued time period, and is time constant since it did not consider the at time information, for instance, the sudden storm or the influence from the drought response actions in this process.

This study provides a new solution to the problems of low reliability and flexibility for early stage drought warning and high time delay of drought response in drought management. In this paper, the whole drought process is divided into four stages by using SPI, and a new dynamic identification mechanism based on the division of drought stages is proposed, which can effectively advance the preparation time for drought response. In addition, the new mechanism closely integrates historical evaluation information, real-time feedback information and predicted future information, to closely track the development of the drought, and take various drought relief actions in time to reduce the economic losses and negative effects.

2. METHODS

2.1. Study area and data

This paper selects Yulin City in northern Shaanxi, China as the research area. Yulin City is located in the northern part of Shaanxi Province, between 107° 28′–111° 15′ east longitude and 36 °57′–39 °35′ north latitude. The area is 385 km long from east to west and 263 km wide from north to south, covering a total area of 43,578 km^2, with an average annual rainfall of 407.7 mm and very scarce water resources per capita. Figure 1 shows an overview of the entire study area.

The data is the rainfall data from 1955 to 2019 at Yulin Meteorological Station (East longitude: 109 °78′, North latitude: 38 °27′), from the National Meteorological Information Center (NMIC) (available at http://data.cma.cn/). In addition, the rainfall data has undergone strict quality inspection by NMIC before release, including the reliability, homogeneity and consistency of the data, and the data quality performance is excellent.

The inter and intra-annual variation of rainfall in Yulin from 1955 to 2019 are shown in Figure 2. From Figure 2(a), the average rainfall in Yulin from 1955 to 2019 was 407.7 mm, with the largest annual rainfall in 2016 (724.9 mm) and the smallest annual rainfall in 1965 (143.3 mm). The extreme value ratio is as high as 5.06, indicating its high inter-annual variability in rainfall. Judging from the change trend, there is no obvious stage change trend of rainfall in Yulin, with a fluctuating decreasing trend before 2000 and a fluctuating increasing trend after 2000. The overall trend is increasing. From Figure 2(b), the annual distribution of rainfall in Yulin is extremely uneven, mainly concentrated in summer, accounting for 61.9% of the

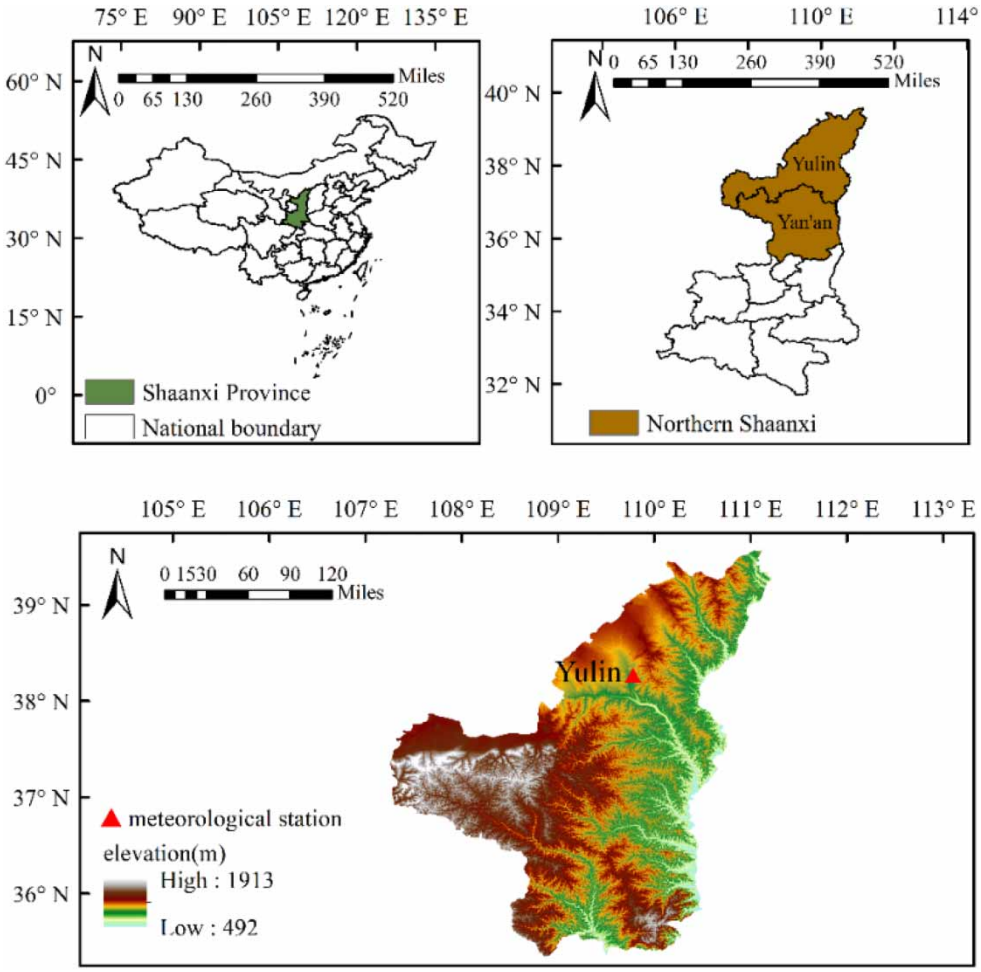

Figure 1 | Location of study area and Yulin meteorological station.

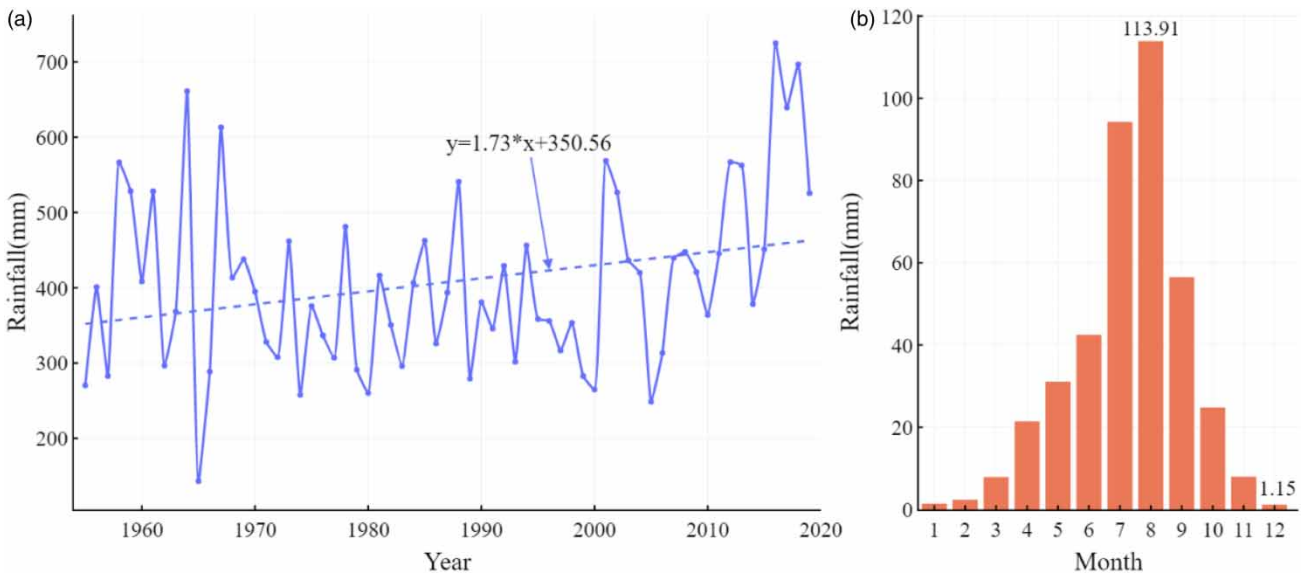

Figure 2 | Inter-annual and intra-annual variation of rainfall in Yulin City from 1955 to 2019. (a) Variation trend of annual rainfall in Yulin City from 1955 to 2019. (b) Average monthly rainfall in Yulin City from 1955 to 2019.

annual rainfall. The average rainfall in August is the largest (113.91 mm), accounting for 28.12% of the annual average rainfall; the average rainfall in December is the smallest (1.15 mm), accounting for only 0.28% of the annual average rainfall.

2.2. Process description of drought events

Drought is a gradual disaster, which usually lasts for months or even years, and its essence is a long-term physical accumulation and restoration process. Assuming a unit of days, the drought degree of each day from the beginning to the end of a drought event can be expressed as the time series $D = (d_1, d_2, \cdots, d_n)$. Therefore, we can do the analysis at both micro and macro scales, and the flow chart is shown in Figure 3.

First, the analysis is done on a micro scale, by considering each day of the drought event as an impact factor and combining it with the two adjacent days before and after to form a module of three consecutive days. Then the physical evolution process of the drought event from the beginning to the end is shown in Figure 4.

From Figure 4, in the module (*day 1*) formed by d_1, the drought situation of the day (d_1) was not only affected by the accumulation and decline of the drought on the previous day (d_0), but also affected the change trend of the drought on the following day (d_2). When the end of the first day enters the module (*day 2*) formed by d_2, due to the influence of clustering behavior (or else Hurst phenomenon by Hurst 1951; Tong *et al.* 2018) from drought, the interaction relationship between d_1, d_2, and d_3 in the '*day 2*'module is consistent with that in the '*day 1*' module (Dimitriadis *et al.* 2021). This interaction

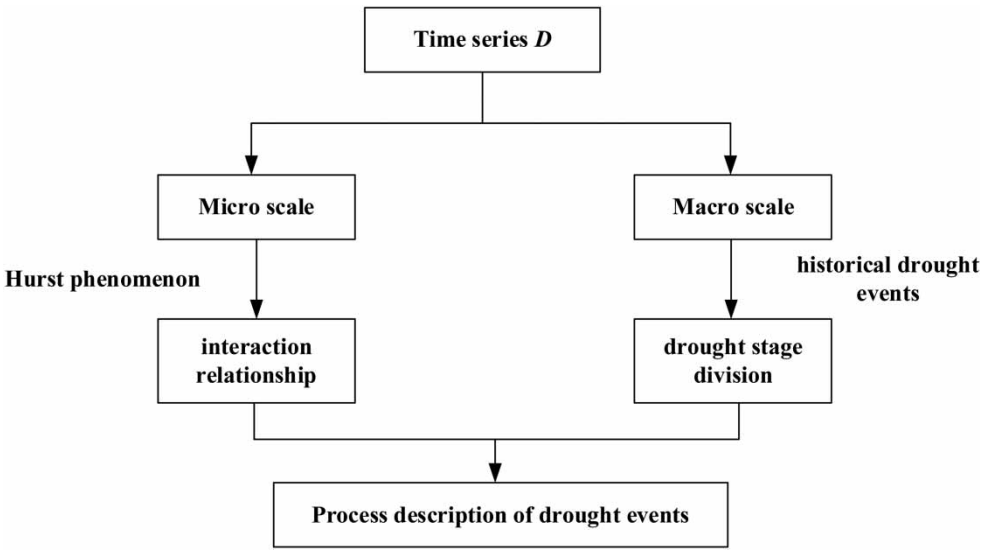

Figure 3 | Flow chart of drought event process analysis.

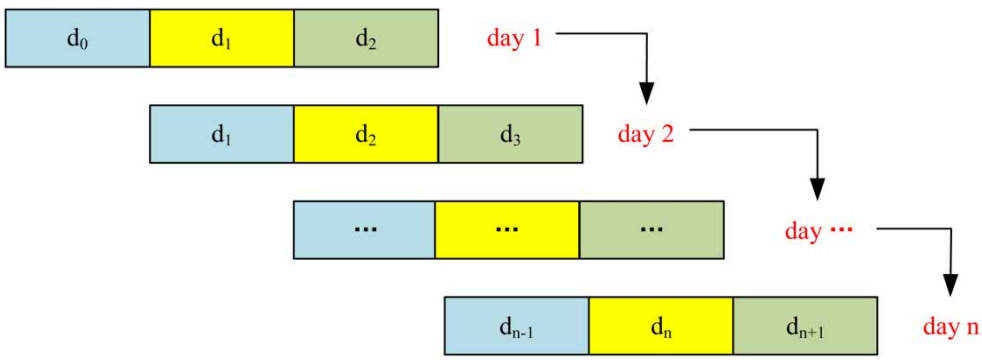

Figure 4 | Schematic diagram of the daily time scale evolution of drought events.

continued to the module (*day n*) formed by d_n on the last day of drought. This characteristic of drought is actually the well-known Hurst phenomenon (Habib 2020). It reflects the result of a long series of interrelated events. What happens today will affect the future, and what happened in the past will affect the present (Shi *et al.* 2021). The periodic continuous physical changes of drought on the time axis can be described as the process of drought events.

Secondly, from the macro scale analysis, all the points in the time series D are connected in sequence to form a complete timeline of the occurrence and development of drought events. By collecting some typical drought events in history we find that the duration and extent of drought varies from one drought event to another, and it is not possible to quantify the course of all drought events in a uniform manner. However, all drought event processes can be roughly divided into two parts: cumulative rise and restoration fall. On this basis, this article further divides these two parts into four stages: accumulation period, outbreak period, reaction period, and restoration period, and this drought event timeline composed of time series D can be represented by Figure 5.

The horizontal axis in Figure 5 is time, and the unit can be days, 10 days, months or even years, and the vertical axis is the degree of drought. Points a, b, c, d, e, and f represent the identification work done throughout the drought event. The points t_1, t_2, and t_3 represent the turning time points between the four stages, and these three turning points (t_1, t_2, and t_3) can be determined according to the calculation results of the drought index. This study selects the drought index SPI (McKee *et al.* 1993) as an example for illustration. SPI is widely used in drought analysis because of the characteristics of simple calculation data and multiple time scales (Eris *et al.* 2020). The SPI formula is given by Equation (1):

$$SPI = S\frac{t-(c_2t+c_1)t+c_0}{((d_3+d_2)t+d_1)t+1.0} \tag{1}$$

where the expression form of t is $t = (\ln(1/P^2))^{1/2}$, P is the cumulative probability of rainfall on a given time scale, and when $P > 0.5$, $P = 1.0-P$ and $S = 1$; when $P \leq 0.5$, $S = -1$.

In the equations above, $c_0 = 2.515517$, $c_1 = 0.802853$, $c_2 = 0.010328$, $d_1 = 1.432788$, $d_2 = 0.189269$ and $d_3 = 0.001308$.

According to the existing related research (Bouaziz *et al.* 2021) and the research on SPI index in Yulin area (Kong *et al.* 2021), the SPI drought classification standard is shown in Table 1.

2.2.1. Drought accumulation period

The data used in the current SPI calculation is the monthly accumulated rainfall, and most of them are identified and calculated once at the end of each month, that is, the frequency of drought identification is on a monthly scale. During the period before point t_1, the SPI value obtained by the identification and calculation for consecutive months showed a continuous downward trend, but the minimum value did not drop below −0.5, and the drought degree was still close to the normal range. Until the next month after the time node t_1 is identified, the SPI value obtained has dropped below −0.5, and at

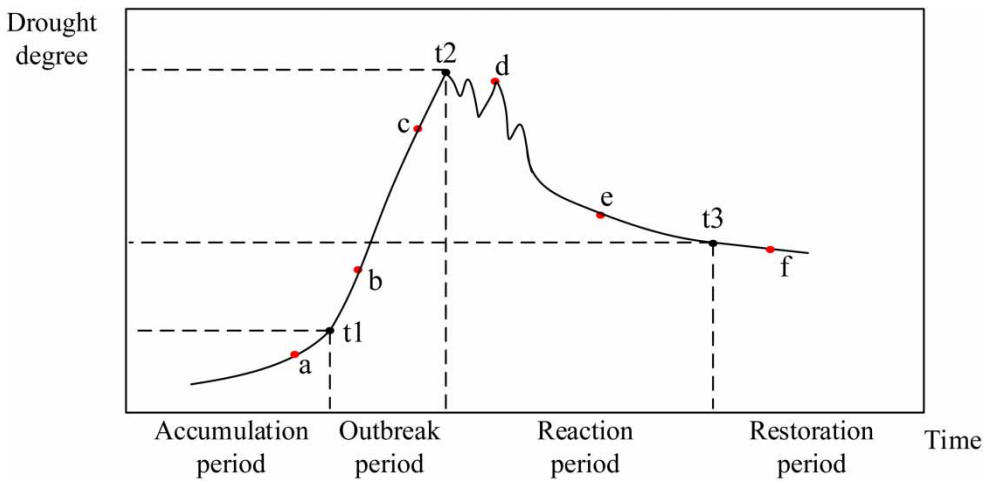

Figure 5 | Schematic diagram of the division of the whole process of the drought event.

Table 1 | SPI drought classification standard

Classification	SPI
Extremely wet (EW)	$SPI > 2.0$
Very wet (VW)	$1.50 < SPI \leq 2$
Moderately wet (MW)	$1.0 < SPI \leq 1.50$
Near normal (NN)	$-0.5 < SPI \leq 1.0$
Light drought (LD)	$-1.0 < SPI \leq -0.5$
Moderate drought (MD)	$-1.50 < SPI \leq -1.0$
Severe drought (SD)	$-2.0 < SPI \leq -1.50$
Extreme drought (ED)	$SPI \leq -2.0$

this time it has risen from no drought to drought. Therefore, the t_1 node is the minimum point where the SPI continues to decline and does not fall below -0.5. The stage before the point t_1 is called the accumulation period of drought.

2.2.2. Drought outbreak period

After several months of accumulation of drought, the quantitative change finally caused the qualitative change. The SPI value will rapidly drop to light drought or even more severe within 1–2 months after point t_1. Therefore, point t_2 is the first point after point t_1, and the period t_1-t_2 is called the drought outbreak period.

2.2.3. Drought reaction period

Drought is a long-term process after all, the SPI value of most drought events will fluctuate up and down after point t_2, and then enter a full-scale recession. Point t_3 is the turning point when SPI rises above -0.5 for the first time during the full-scale recession. The period t_2-t_3 is called the drought reaction period.

2.2.4. Drought restoration period

A few months after point t_3, the SPI rises and returns to a normal state. This stage is called the restoration period of the drought. At this point, a drought event is completely over, human production and life are on the right track again, and the impact is gradually eliminated.

2.3. Dynamic identification mechanism based on drought process

2.3.1. Identification and early warning mechanism based on process

It can be clearly seen from Figure 5 that the drought identification at each stage is based on the drought process, and there are relatively static points on the process line. Therefore, the advantage of the division of the drought process is that through identification, the current stage can be clarified and early warning signals can be issued at the beginning of the stage to carry out corresponding response actions. For example, in the accumulation period, it is necessary to prepare a drought response plan and develop a drought prediction model; in the outbreak period, we should quickly respond to the drought, transfer rescue materials nearby, and give priority to the disaster victims with the most serious water shortage. At the same time, the frequency of monitoring and identification should be appropriately increased to facilitate timely follow-up rescue work. During the reaction period, the deployment of emergency water sources, artificial rainfall, reservoir dispatching and other water resources should be done well, the effectiveness of rescue measures should be evaluated, and the rescue plan should be adjusted in time; During the restoration period, it is necessary to do a good job in post-disaster reconstruction and material replenishment, sum up the experience of drought relief, and organize the resumption of work and production.

2.3.2. Dynamic identification mechanism

In order to give full play to the role of drought identification, this research builds a dynamic identification mechanism that considers drought prediction and feedback information on the basis of information data collection and drought index calculation, so as to realize the close application of historical evaluation information and prediction results. On the one hand, the occurrence of drought can be identified in advance based on the constantly updated basic information during identification,

on the other hand, it can effectively obtain the emergencies between two adjacent identifications and make a quick response. The most critical link in the mechanism is rolling identification and early warning, as shown in Figure 6.

First of all, the drought monitoring department uses advanced data collection methods to obtain the latest basic data such as rainfall, evaporation, and soil moisture during daily identification work. Secondly, select appropriate drought indicators for the monitored drought types, analyze and calculate the current drought degree, and report the identification results to the Drought Relief Headquarters. Then, the Drought Relief Headquarters formulated drought management plans and action plans based on the reported identification results and issued them to the front-line departments for implementation. Finally, the drought monitoring department evaluates the effects of the collected feedback from water users and emergencies, and decides whether it is necessary to immediately carry out drought prediction and carry out the second round of identification work.

2.4. Prediction model development

Machine learning algorithms have been recognized as an effective tool for modeling in the complex hydrology field. The most common algorithm is artificial neural network (ANN). The neural network model with back propagation is used in drought identification and prediction in this paper. However, when SPI time series is used as input, because it is a typical nonlinear and unstable sequence, we use singular spectrum analysis (SSA) to pre-process it and extract the hidden information in the sequence, so that the prediction model can better capture it.

2.4.1. Singular spectrum analysis (SSA)

SSA is a new rising method in recent years to study nonlinear time series data (Yu *et al.* 2017). It can effectively mine the signal information such as periodicity, long-term trend and noise hidden in time series, so as to analyze the structure of time series and further use it for prediction. Assuming that there is a set of one-dimensional time series $(\boldsymbol{x}_1, \boldsymbol{x}_2, \cdots \boldsymbol{x}_N)$, the specific steps for performing SSA on it are as follows:

(1) Embedding. Choosing an appropriate window length L $(1<L<N)$ and transform the one-dimensional time series into a multidimensional time series $\boldsymbol{X_i} = (\boldsymbol{x_i}, \boldsymbol{x_{i+1}}, \cdots, \boldsymbol{x_{i+L-1}})^{\boldsymbol{T}}$, $\boldsymbol{i} = 1, 2, 3, \cdots, \boldsymbol{K}$, where $\boldsymbol{K} = \boldsymbol{N} - \boldsymbol{L} + 1$. Combining all the multidimensional series to obtain the trajectory matrix X as in Equation (2):

$$X = [X_1 : X_2 : \cdots : X_N] = (x_{ij})_{i,j=1}^{L,K} = \begin{bmatrix} x_1 & x_2 & x_3 & \cdots & x_K \\ x_2 & x_3 & x_4 & \cdots & x_{K+1} \\ \vdots & \vdots & \vdots & \ddots & \vdots \\ x_L & x_{L+1} & x_{L+2} & \cdots & x_N \end{bmatrix} \tag{2}$$

The size of the window length L generally does not exceed 1/2 of the length of the one-dimensional time series. If the approximate period of the one-dimensional time series can be determined, L is preferably selected according to an integer

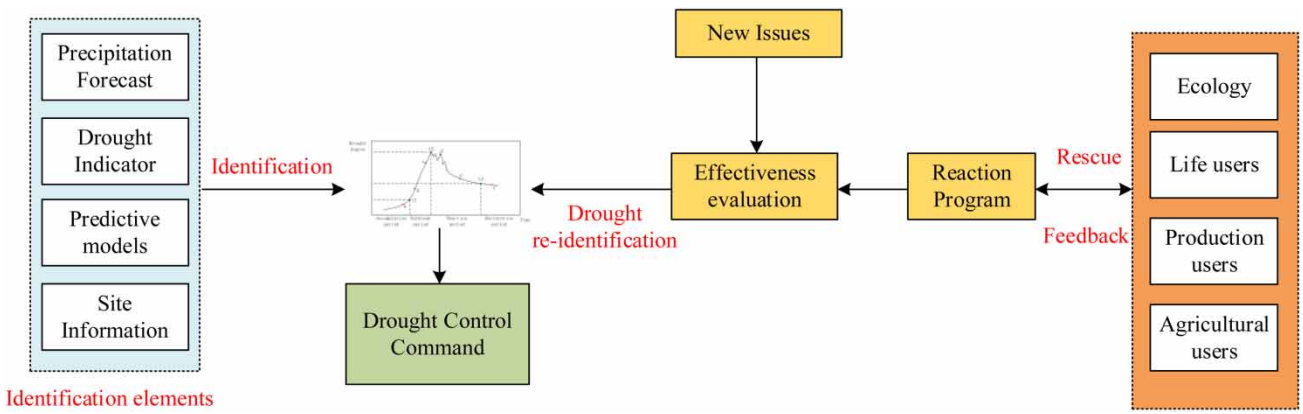

Figure 6 | Schematic diagram of rolling identification warning of drought.

multiple of its period. In this paper, the size of L is set to 12, so the original SPI-12 time series will get 12 components after SSA.

(2) Singular Value Decomposition (SVD). Calculating XX^T and obtain its L eigenvalues $\lambda_1 \geq \lambda_2 \geq \cdots \geq \lambda_L \geq 0$, $U_1, \cdots, U_L$ are their corresponding orthogonal eigenvectors, and $d = max\{i{:}\lambda_i > 0\}$. If we let $V_i = X^T U_i/\sqrt{\lambda_i}(i = 1, \cdots, d)$, then the singular value decomposition of the trajectory matrix X is as Equation (3):

$$X = Y_1 + Y_2 + \cdots + Y_d \tag{3}$$

where $Y_i = \sqrt{\lambda_i} U_i V_i^T$ represents the ith SVD component. In addition, these eigenvalues mainly indicate the importance of each SVD component to the original signal, therefore, the importance of the SVD component to the original signal decreases sequentially as the order increases.

(3) Grouping. Dividing the index set $I = \{1, \cdots, d\}$ into several groups $I_1, \cdots, I_m$, and sum the matrices Y_i in each group. The mathematical expression of the result is as Equation (4):

$$X = \sum_{k=1}^{m} X_{I_k}, \quad \text{where } X_{I_k} = \sum_{i \in I_k} Y_i \tag{4}$$

(4) Reconfiguration. Using the diagonal mean method to calculate the diagonal mean of the matrix X_{I_k}, and convert the matrix X_{I_k} into its corresponding time series data. Each set of time series data presents the hidden properties of the original series, such as long-term trends, periodicity, noise signals, etc. Then the value of the original time series is equal to the summation of each characteristic decomposition sequence, as shown in Equation (5).

$$x_n = \sum_{k=1}^{m} f_n^{(k)}, \; n = 1, 2, \cdots, N \tag{5}$$

where the sequence $f_n^{(k)}$ corresponding to each k is the diagonal mean of the matrix X_{I_k}.

2.4.2. Back propagation neural network (BPNN)

BPNN is a multi-layer feedforward network trained by the error back-propagation algorithm, and it is one of the most widely used neural network models. The BP network can learn and store a large number of input-output pattern mapping relationships without revealing the mathematical equations describing this mapping relationship in advance. Its neurons are arranged in layers, consisting of input layer, hidden layer and output layer, of which the hidden layer may have multiple layers (Liu *et al.* 2020). This paper uses a three-layer BPNN, and its network structure is shown in Figure 7.

Each neuron in the input layer is responsible for receiving input information from the outside world and passing it to each neuron in the hidden layer. The hidden layer is the internal information processing layer, responsible for information transformation. The output layer receives the information transmitted by the hidden layer, and after further processing, outputs the information processing results to the outside world, and completes a learning forward propagation process. When the actual output does not match the expected output, it enters the back-propagation stage of the error. The error is back-propagated layer by layer through the output layer, correcting the weights of each layer in an error gradient descent manner, towards the hidden and input layers.

2.4.3. The flow of SSA-BPNN model prediction

The SSA-BPNN prediction model is a new type of hybrid prediction model, and its specific prediction process is shown in Figure 8. The prediction process is roughly divided into the following three steps:

(1) The original time series of the observed SPI-12 can be obtained through the measured monthly rainfall data.
(2) Selecting the appropriate window length ($L = 12$) and performing singular spectrum analysis on the original SPI-12 time series to extract the hidden information in the original time series and reduce the influence of noise.
(3) The 12 components obtained by singular spectrum analysis are respectively brought into the BPNN model for prediction, and then the predicted values of the 12 components are summed to obtain the predicted value of SPI-12.

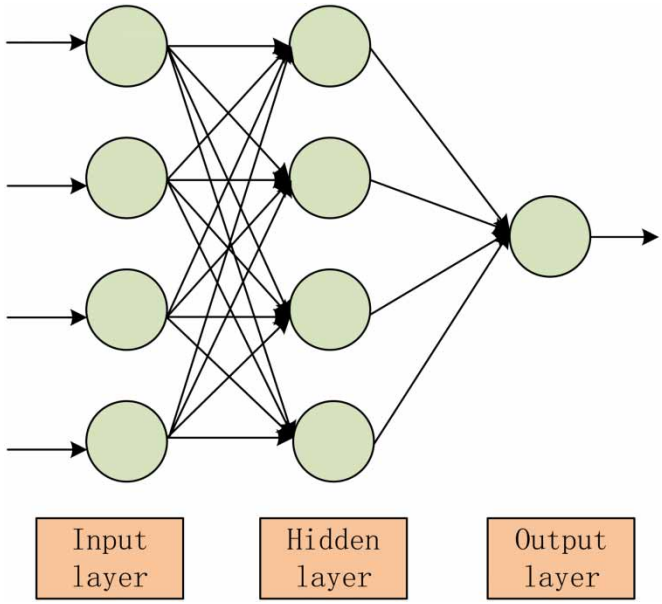

Figure 7 | Three-layer BP neural network structure diagram.

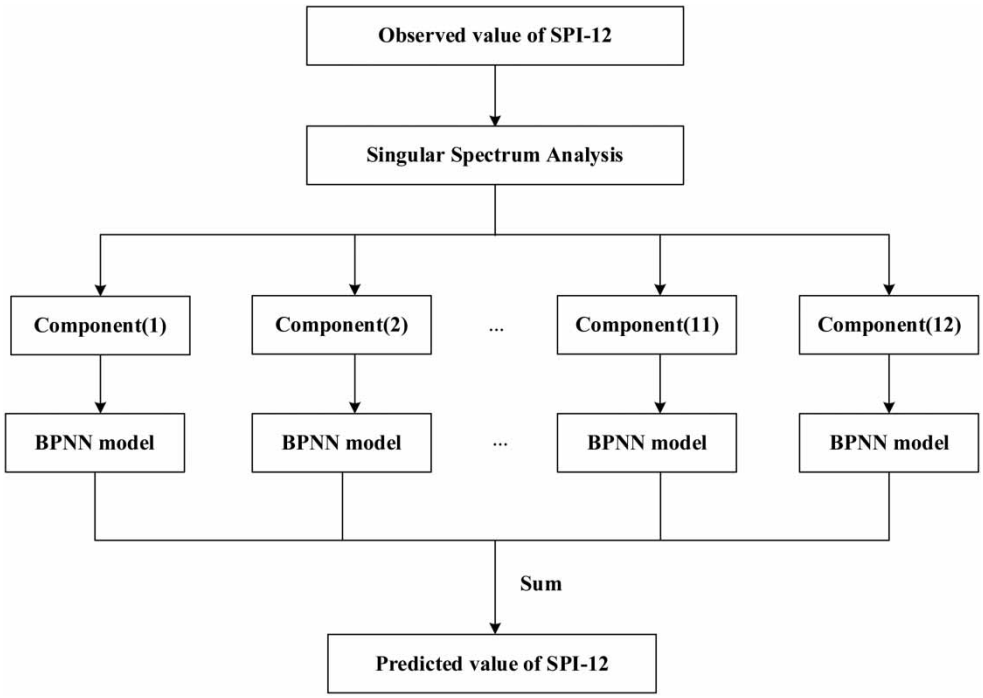

Figure 8 | SSA-BPNN model prediction flow chart.

3. CASE STUDY AND RESULT

In this study, three drought events in recent years in Yulin, northern Shaanxi, China, were taken as examples, and the dynamic identification mechanism based on the drought event process was used to simulate them respectively.

Case Simulation 1 (May 2005 to July 2007):

Drought accumulation period: When the Yulin Hydrological Bureau did daily drought identification calculations at the end of July 2005, the SPI-12 obtained was greater than −0.5, which was within the normal range and no drought occurred. However, through the feedback channel of the identification mechanism, the Meteorological Department informed that next month's rainfall will be much lower than the same period, and there may be droughts. Therefore, the Hydrological Bureau used the prediction model SSA-BPNN to predict SPI-12 of Yulin Meteorological Station from May 2005 to July 2007. The model prediction results are shown in Figure 9.

From Figure 9, the Yulin Hydrological Bureau's prediction of SPI-12 for August 2005 at *t2* is −1.1, indicating that a moderate drought will occur in August. The Bureau of Hydrology immediately issued a drought warning signal and reported the results to the Drought Relief Headquarters to prepare a drought relief plan. According to the method of determining the drought stage proposed in the second section of this article, it can be concluded that the accumulation period of this drought event is from May 2005 to July 2005. During this period, SPI-12 showed a continuous downward trend, and the minimum value appeared at *t1* of −0.04.

Drought outbreak period: In August 2005, the observed value of SPI-12 in Yulin was between −1.5 and −2.0, indicating a severe drought in the area. However, according to the drought identification and warning results reported by the Hydrological Bureau, the Drought Relief Headquarters had made arrangements in advance, and had taken emergency measures to start rescue operations at the beginning of the month. From Figure 9, the predicted and actual values of SPI from July 2005 to August 2005 have the same trend, and both have increased from no drought to drought. Therefore, the outbreak period of this drought event is August 2005. During this period, the Drought Relief Headquarters not only called in nearby materials, but also organized an expert consultation meeting to comprehensively study and judge future drought trends and prepare for long-term drought relief.

Drought reaction period: At the beginning of September 2005, after consultation with experts, a new action plan was formulated and issued to all action departments involved in the rescue. After the water users received relevant rescues, they would feed back to the rescue operations department whether the drought was alleviated. At the same time, new problems will also arise during the rescue period, such as sudden rainstorms, whether the use of emergency water sources is effective, and whether the number of artificial rainfall is sufficient. The Hydrological Bureau collects and evaluates the feedback information and new problems through the identification mechanism. On the basis of the evaluation results, continue to carry out rolling identification and early warning, and continuously report the newly identified results to the drought control

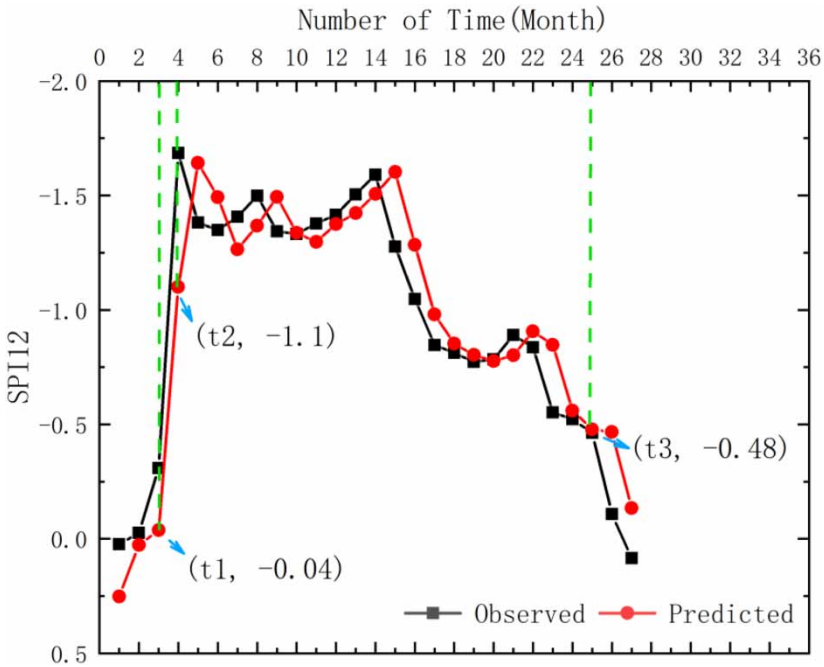

Figure 9 | Drought prediction model results from May 2005 to July 2007.

headquarters to ensure that the deployment of water resources can keep up with the development of drought. In July 2006, after 11 months of ups and downs, the drought finally entered a full recession. From Figure 9, the prediction results show that SPI-12 has been rising in general since July 2006, and it rose to −0.48 at *t3* in May 2007, returning to normal. Therefore, the period from September 2005 to May 2007 is the reaction period for this drought event.

Drought restoration period: After more than a year of drought response, the drought completely ended in May 2007. Therefore, the restoration period of this drought event was June 2007 to July 2007. During these two months, the relevant departments organized the aftermath, guided the supplement of emergency supplies, promoted the recovery of production and life after the disaster, carried out post-disaster work evaluation, summed up experience and lessons, and put the files in the database to provide reference for subsequent drought relief. At the same time, the Hydrological Bureau restored the normal frequency of drought identification to ensure the reasonable allocation and use of manpower and material resources.

Case Simulation 2 (November 2010 to November 2011) and Case Simulation 3 (November 2014 to October 2015):

In cases 2 and 3, the SPI-12 observed values of the Hydrological Bureau for several consecutive months showed a continuous downward trend. Therefore, the Hydrological Bureau judged that there would be a drought, so the drought prediction work was started in time, and the prediction results of the SSA-BPNN model for cases 2 and 3 are shown in Figures 10 and 11, respectively.

From Figure 10, the SPI-12 predicted by the Hydrology Bureau at *t2* (April 2011) was −0.56, while the SPI-12 at *t1* (March 2011) was −0.25. Therefore, according to the method for determining the drought stage proposed above, the drought accumulation period of case 2 is from November 2010 to March 2011. After the drought event, the follow-up actions in case 2 were the same as in case 1, so according to Figure 10, it can be seen that the drought outbreak period of case 2 was April 2010. The predicted SPI-12 at *t3* (August 2011) was 0.22 and the subsequent SPI-12 values were all greater than −0.5, marking the end of this drought event. From this, it can be obtained that the drought reaction period of case 2 is from May 2011 to August 2011, and the drought restoration period is from September 2011 to November 2011.

Using the same reasoning, according to Figure 11, the duration of each stage of case 3 is directly given. The drought accumulation period was from November 2014 to May 2015, the drought outbreak period was from June 2015, the drought reaction period was from July 2015 to August 2015, and the drought restoration period was from September 2015 to October 2015.

In the simulation process of cases 2 and 3, the drought reaction period and drought restoration period judged by the prediction results have a one-month error compared with the actual process. This is mainly because the sudden increase in the

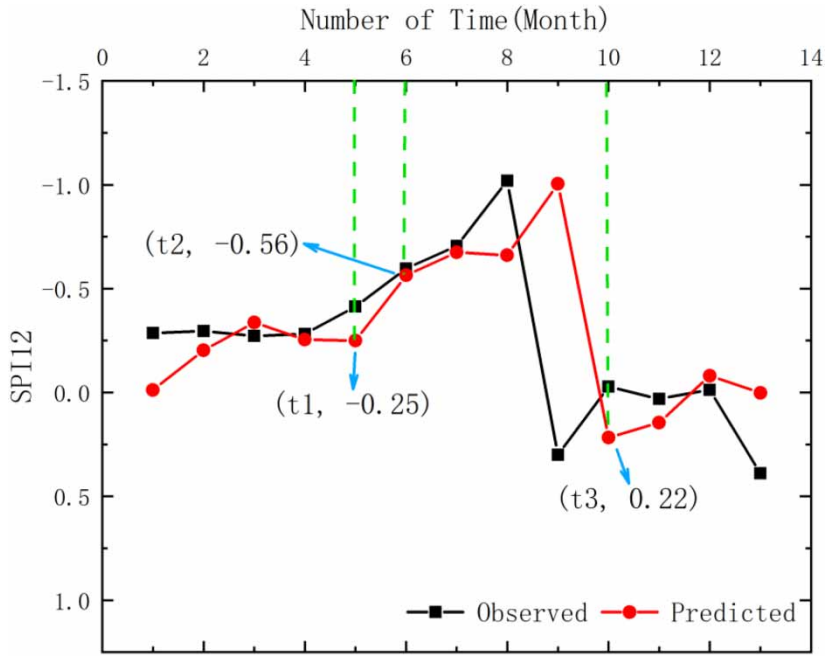

Figure 10 | Drought prediction model results from November 2010 to November 2011.

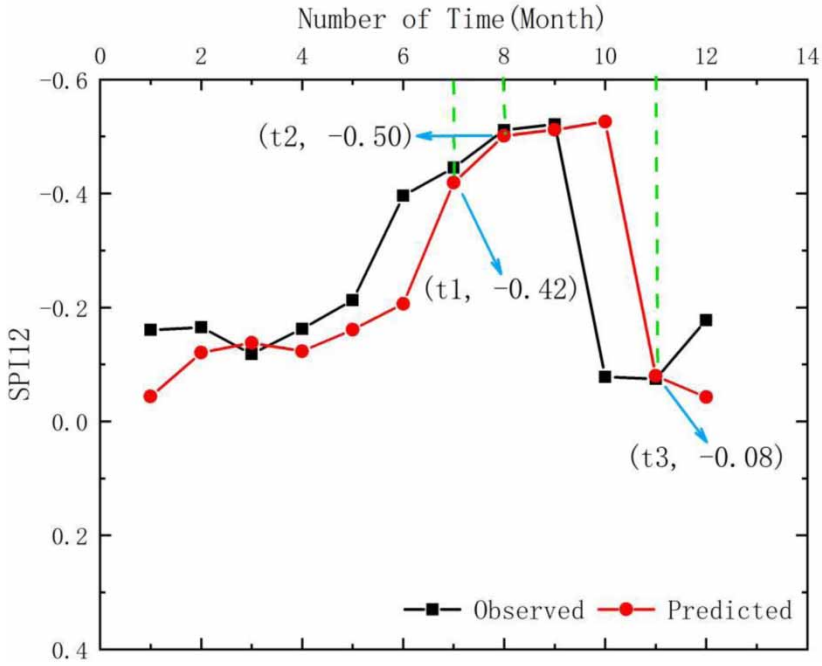

Figure 11 | Drought prediction model results from November 2014 to October 2015.

cumulative rainfall of the month has a decisive impact on the relief of the drought, which makes the SPI-12 value rise too fast, resulting in the prediction model failing to capture the sudden changes in time and producing certain prediction errors. However, this error has little effect on a drought that lasts for more than one year, because the drought occurrence and development trend we simulated and plotted in advance is highly consistent with the actual situation, so effective response measures have been carried out at each stage.

4. DISCUSSION

Compared with case 1, cases 2 and 3 have shorter duration and less degree of drought, which verifies the point of Section 2 that the duration and intensity of drought events are difficult to quantitatively express uniformly. However, they all experience two main processes of cumulative rise and restoration fall. On this basis, the research on the division of drought stages has high application value. In the past, the research on the division of drought stages basically started after the occurrence of drought. As a result, most of the time we can only passively resist drought, and even no effective measures were taken after the drought. The identification and early warning of drought lags behind the development of drought, which brings a lot of unnecessary economic losses. Bandyopadhyay *et al.* (2020) pointed out that most of the existing drought policies are passive in nature. In addition, the guidelines for each stage of drought management must be strong specific drought policies proposed by the country, and the focus of drought policy should be on preparation for future droughts of any intensity, frequency and duration. An important contribution of this paper is that the proposed four-stage division of drought includes the new concept of drought accumulation period, which can effectively advance the preparation time for early drought resistance and do sufficient mobilization work, thereby changing passive drought resistance to active drought resistance. At the same time, a clear division of drought stages is more conducive to the implementation and adjustment of drought policies.

In addition, Brockhoff *et al.* (2022) used a new mechanism-based approach to analyze the future of the Dutch drought governance system, and argued that multifaceted research on mechanisms can accelerate and guide future management of drought. The new dynamic identification mechanism based on the drought process proposed in this paper can combine the historical evaluation of drought with real-time feedback information, closely track the development trend of drought and improve the timeliness of drought action. Moreover, the maximum value of such a high-precision prediction model as SSA-BPNN can be fully utilized to provide new management ideas and operation methods for comprehensive drought

disaster fighting, and solve the problem of poor integration between scientific research and practical application. This is rarely mentioned in the previous drought research.

5. CONCLUSION

From the drought management expectation, in this study, the drought event is identified as a process according to the SPI value, and the warnings vary with time by considering the prediction and the influence from the drought response actions. Validated by the application case study, the following conclusions can be achieved:

(1) Considering drought as a process rather than a whole event could capture more valuable information for drought identification;
(2) Drought warning should change with timely updated conditions in the drought process, rather than only the historical information;
(3) The division of drought stage can effectively advance the preparation time for drought response and help to order the reactions in drought responses.

The above conclusions are deduced based on the content of current study, and more work could be done in the future. Such as:

(1) In the selection of drought indexes, we used SPI in this article. In the future, we will try more drought indexes to study the drought process. In particular, some multi-variate standardized indexes, such as PDSI, SPEI, etc., can be used to assist in judging the different stages of drought events.
(2) Hurst index has been proved to be effective in improving drought prediction level and contributing to the trend analysis of the drought process. In subsequent research, we will try to consider introducing the Hurst index into the division of drought process and the construction of a drought prediction model, to further improve its rationality and reliability.

ACKNOWLEDGEMENTS

This work was supported by the Natural Science Basic Research Program of Shaanxi Province (Grant No. 2019JLZ-16). The authors thank the editor for their comments and suggestions.

DATA AVAILABILITY STATEMENT

All relevant data are included in the paper or its Supplementary Information.

CONFLICT OF INTEREST

The authors declare there is no conflict.

REFERENCES

Ali, Z., Hussain, I., Faisal, M., Almanjahie, I. M., Ahmad, I., Khan, D. M., Grzegorczyk, M. & Qamar, S. 2019 A probabilistic weighted joint aggregative drought index (PWJADI) criterion for drought monitoring systems. *Tellus A: Dynamic Meteorology and Oceanography* **71** (1), 1588584. doi:10.1080/16000870.2019.1588584.

Altunkaynak, A. & Jalilzadnezamabad, A. 2021 Extended lead time accurate forecasting of palmer drought severity index using hybrid wavelet-fuzzy and machine learning techniques. *Journal of Hydrology* **601**, 126619. doi:10.1016/j.jhydrol.2021.126619.

Bandyopadhyay, N., Bhuiyan, C. & Saha, A. K. 2020 Drought mitigation: critical analysis and proposal for a new drought policy with special reference to Gujarat (India). *Progress in Disaster Science* **5**, 100049. doi:10.1016/j.pdisas.2019.100049.

Berliana, S., Susanti, I., Siswanto, B., Nurlatifah, A., Latifah, H., Witono, A., Slamet, L. & Suhermat, M. 2021 Analysis of wet and dry season by using the Palmer Drought Severity Index (PDSI) over Java Island. In *AIP Conference Proceedings*, pp. 030010. doi:10.1063/5.0041843.

Bouaziz, M., Medhioub, E. & Csaplovisc, E. 2021 A machine learning model for drought tracking and forecasting using remote precipitation data and a standardized precipitation index from arid regions. *Journal of Arid Environments* **189**, 104478. doi:10.1016/j.jaridenv.2021.104478.

Brockhoff, R. C., Biesbroek, R. & Van der Bolt, B. 2022 Drought governance in transition: a case study of the Meuse River Basin in the Netherlands. *Water Resources Management* 1–16. doi:10.1007/s11269-022-03164-7.

Cai, X. H., Zhang, W. Q., Fang, X. Y., Zhang, Q., Zhang, C. J., Chen, D., Cheng, C., Fan, W. J. & Yu, Y. 2021 Identification of regional drought processes in North China using MCI analysis. *Land* **10** (12), 1390. doi:10.3390/land10121390.

Dar, J. & Dar, A. Q. 2021 Spatio-temporal variability of meteorological drought over India with footprints on agricultural production. *Environmental Science and Pollution Research* **2**, 1–14. doi:10.1007/s11356-021-14866-7.

Dimitriadis, P., Koutsoyiannis, D., Iliopoulou, T. & Papanicolaou, P. 2021 A global-scale investigation of stochastic similarities in marginal distribution and dependence structure of key hydrological-cycle processes. *Hydrology* **8** (2), 59. doi:10.3390/hydrology8020059.

Ding, Y. B., Gong, X. L., Xing, Z. X., Cai, H. J., Zhou, Z. Q., Zhang, D. D., Sun, P. & Shi, H. Y. 2021 Attribution of meteorological, hydrological and agricultural drought propagation in different climatic regions of China. *Agricultural Water Management* **255**, 106996. doi:10.1016/j.agwat.2021.106996.

Eris, E., Cavus, Y., Aksoy, H., Burgan, H. I., Aksu, H. & Boyacioglu, H. 2020 Spatiotemporal analysis of meteorological drought over Kucuk Menderes River Basin in the aegean region of Turkey. *Theoretical and Applied Climatology* **142** (3), 1515–1530. doi:10.1007/s00704-020-03384-0.

Ghasemi, P., Karbasi, M., Nouri, A. Z., Tabrizi, M. S. & Azamathulla, H. M. 2021 Application of Gaussian process regression to forecast multi-step ahead SPEI drought index. *Alexandria Engineering Journal* **60** (6), 5375–5392. doi:10.1016/j.aej.2021.04.022.

Habib, A. 2020 Exploring the physical interpretation of long-term memory in hydrology. *Stochastic Environmental Research and Risk Assessment* **34** (12), 2083–2091. doi:10.1007/s00477-020-01883-0.

Hurst, H. E. 1951 Long-term storage capacity of reservoirs. *Transactions of the American Society of Civil Engineers* **116** (1), 770–799. doi:10.1061/TACEAT.0006518.

Javed, T., Yao, N., Chen, X. G., Suon, S. & Li, Y. 2020 Drought evolution indicated by meteorological and remote-sensing drought indices under different land cover types in China. *Environmental Science and Pollution Research* **27** (4), 4258–4274. doi:10.1007/s11356-019-06629-2.

Kogan, F. N. 1990 Remote sensing of weather impacts on vegetation in non-homogeneous areas. *International Journal of Remote Sensing* **11=**(8), 1405–1419. doi:10.1080/01431169008955102.

Kolachian, R. & Saghafian, B. 2021 Hydrological drought class early warning using support vector machines and rough sets. *Environmental Earth Sciences* **80** (11), 1–15. doi:10.1007/s12665-021-09536-3.

Kong, G., Zhang, S. L., Wang, L., Huang, S. Z. & Bai, J. Y. 2021 Temporal-spatial evolution of drought characteristics at different grades in Yulin. *Pearl River* **42** (11), 29–37. doi:10.3969/j.issn.1001-9235.2021.11.005.

Kundu, A., Dutta, D., Patel, N. R., Denis, D. M. & Chattoraj, K. K. 2021 Evaluation of socio-economic drought risk over bundelkhand region of India using analytic hierarchy process (AHP) and geo-spatial techniques. *Journal of the Indian Society of Remote Sensing* **49** (6), 1–13. doi:10.1007/s12524-021-01306-9.

Liu, X. F., Zhu, X. F., Zhang, Q., Yang, T. T., Pan, Y. Z. & Sun, P. 2020 A remote sensing and artificial neural network-based integrated agricultural drought index: index development and applications. *Catena* **186**, 104394. doi:10.1016/j.catena.2019.104394.

Marini, G., Fontana, N. & Mishra, A. K. 2019 Investigating drought in apulia region, Italy using SPI and RDI. *Theoretical and Applied Climatology* **137** (1), 383–397. doi:10.1007/s00704-018-2604-4.

McKee, T. B., Doesken, N. J. & Kleist, J. 1993 The relationship of drought frequency and duration to time scales. In *Proceedings of the 8th Conference on Applied Climatology*, pp. 179–183.

Nasir, H. N. & Hamdan, A. N. A. 2021 Short-term and Long-term Drought Forecasts in Iraq Using Neural Networks and GIS. In *IOP Conference Series: Materials Science and Engineering*, pp. 012112. doi:10.1088/1757-899X/1090/1/012112.

Nikbakht, J., Tabari, H. & Talaee, P. H. 2013 Streamflow drought severity analysis by percent of normal index (PNI) in northwest Iran. *Theoretical and Applied Climatology* **112** (3), 565–573. doi:10.1007/s00704-012-0750-7.

Palmer, W. C. 1965 *Meteorological Drought*. U.S. Weather Bureau, Research Paper No 45, p. 58. https://www.ncdc.noaa.gov/tempand-precip/drought/docs/palmer.pdf (accessed February 2022).

Pramudya, Y. & Onishi, T. 2018 Assessment of the standardized precipitation index (SPI) in Tegal City, Central Java, Indonesia. In *IOP Conference Series: Earth and Environmental Science*, p. 012019.

Shi, W. Z., Huang, S. Z., Liu, D. F., Huang, Q., Han, Z. M., Leng, G. Y., Wang, H., Liang, H., Li, P. & Wei, X. T. 2021 Drought-flood abrupt alternation dynamics and their potential driving forces in a changing environment. *Journal of Hydrology* **597**, 126179. doi:10.1016/j.jhydrol.2021.126179.

Shin, J. Y., Kwon, H. H., Lee, J. H. & Kim, T. W. 2020 Probabilistic long-term hydrological drought forecast using Bayesian networks and drought propagation. *Meteorological Applications* **27** (1), e1827. doi:10.1002/met.1827.

Singh, O., Saini, D. & Bhardwaj, P. 2021 Characterization of meteorological drought over a dryland ecosystem in north western India. *Natural Hazards* **109** (1), 785–826. doi:10.1007/s11069-021-04857-9.

Sridhara, S., Chaithra, G. M. & Gopakkali, P. 2021 Assessment and monitoring of drought in Chitradurga district of Karnataka using different drought indices. *Journal of Agrometeorology* **23** (2), 221–227. doi:10.54386/jam.v23i2.72.

Sutanto, S. J., Wetterhall, F. & Van Lanen, H. A. 2020 Hydrological drought forecasts outperform meteorological drought forecasts. *Environmental Research Letters* **15** (8), 084010. doi:10.1088/1748-9326/ab8b13.

Tong, S., Lai, Q., Zhang, J., Bao, Y., Lusi, A., Ma, Q., Li, X. & Zhang, F. 2018 Spatiotemporal drought variability on the Mongolian Plateau from 1980–2014 based on the SPEI-PM, intensity analysis and Hurst exponent. *Science of the Total Environment* **615**, 1557–1565. doi:10.1016/j.scitotenv.2017.09.121.

Tsakiris, G. & Vangelis, H. J. E. W. 2005 Establishing a drought index incorporating evapotranspiration. *European Water* **9** (10), 3–11.

Tucker, C. J. 1979 Red and photographic infrared linear combinations for monitoring vegetation. *Remote Sensing of Environment* **8** (2), 127–150. doi:10.1016/0034-4257(79)90013-0.

Vicente-Serrano, S. M., Azorin-Molina, C., Sanchez-Lorenzo, A., Revuelto, J., López-Moreno, J. I., González-Hidalgo, J. C., Moran-Tejeda, E. & Espejo, F. 2014 Reference evapotranspiration variability and trends in Spain, 1961–2011. *Global and Planetary Change* **121**, 26–40. doi:10.1016/j.gloplacha.2014.06.005.

Wang, X. Y., Hao, Y., Hu, J. N., Li, F. & Yu, D. 2021 Recognitions of meteorological drought process and charactistic analysis on disaster causing factors. *Acta Agrestia Sinica* **29** (S1), 35–42. doi:10.11733/j.issn.1007-0435.2021.Z1.005.

Wu, H., Hayes, M. J., Weiss, A. & Hu, Q. 2001 An evaluation of the standardized precipitation index, the China-Z index and the statistical Z-Score. *International Journal of Climatology* **21** (6), 745–758. doi:10.1002/joc.658.

Yu, C. J., Li, Y. L. & Zhang, M. J. 2017 An improved wavelet transform using singular spectrum analysis for wind speed forecasting based on elman neural network. *Energy Conversion and Management* **148**, 895–904. doi:10.1016/j.enconman.2017.05.063.

Yun, S., Jun, Y. & Hong, S. 2012 Social perception and response to the drought process: a case study of the drought during 2009–2010 in the Qianxi'nan Prefecture of Guizhou Province. *Natural Hazards* **64** (1), 839–851. doi:10.1007/s11069-012-0274-6.

Zargar, A., Sadiq, R., Naser, B. & Khan, F. I. 2011 A review of drought indices. *Environmental Reviews* **19** (NA), 333–349. doi:10.1139/A11-013.

Zhang, Y., Hao, Z. C., Feng, S. F., Zhang, X., Xu, Y. & Hao, F. H. 2021 Agricultural drought prediction in China based on drought propagation and large-scale drivers. *Agricultural Water Management* **255**, 107028. doi:10.1016/j.agwat.2021.107028.

First received 29 May 2022; accepted in revised form 19 August 2022. Available online 29 August 2022